Biomaterials Science

ROYAL SOCIETY OF CHEMISTRY

PAPER

View Article Online
View Journal | View Issue

Cite this: *Biomater. Sci.*, 2020, **8**, 3392

A transport system based on a quantum dot-modified nanotracer is genetically and developmentally stable in pregnant mice†

Hye Jin Kim,‡[a] Ji Sun Park,‡[a] Se Won Yi,‡[a] Minyeon Go,[b] Hye-Ryun Kim,[c] Su Jin Lee,[a] Jong Min Park,[a] Dong Hyun Cha,*[d] Sung Han Shim*[b,e] and Keun-Hong Park *[a]

The use of nanoscale materials (NMs) could cause problems such as cytotoxicity, genomic aberration, and effects on human health, but the impacts of NM exposure during pregnancy remain uncharacterized in the context of clinical applications. It was sought to determine whether nanomaterials pass through the maternal–fetal junction at any stage of pregnancy. Quantum dots (QDs) coated with heparinized Pluronic 127 nanogels and polyethyleneimine (PEI) were administered to pregnant mice. The biodistribution of QDs, as well as their biological impacts on maternal and fetal health, was evaluated. Encapsulation of QDs with a nanogel coating produces a petal-like nanotracer (PNt), which could serve as a nano-carrier of genes or drugs. PNts were injected through the tail vein and accumulated in the liver, kidneys, and lungs. QD accumulation in reproductive organs (uterus, placenta, and fetus) differed among phases of pregnancy. In phase I (7 days of pregnancy), the QDs did not accumulate in the placenta or fetus, but by phase III (19 days) they had accumulated at high levels in both tissues. Karyotype analysis revealed that the PNt-treated pups did not have genetic abnormalities when dams were treated at any phase of pregnancy. PNts have the potential to serve as carriers of therapeutic agents for the treatment of the mother or fetus and these results have a significant impact on the development and application of QD-based NPs in pregnancy.

Received 26th February 2020,
Accepted 22nd April 2020

DOI: 10.1039/d0bm00311e

rsc.li/biomaterials-science

1. Introduction

During pregnancy, problematic conditions may arise in the mother, fetus, or both, requiring treatment to cure the disorders or alleviate their symptoms. For example, the mother may experience anemia, hypertension, diabetes, urinary tract infections (UTIs), thromboembolic disorders, or infection by various viruses (pneumonia, HIV, or hepatitis).[1–5] In addition, fetopathy can arise due to innate (genetic) or prenatal (virus, drugs, or various chemicals from the mother) factors.[4–7] Therefore, it is necessary to establish a system for curing diseases in the mother and/or fetus without causing side effects in either. Many highly effective drugs have been developed as therapeutic agents for use in clinical applications.[8–10] However, the short serum half-life and poor bioavailability of many drugs delivered *via* oral or injected routes require frequent administration.[9,11–13] Moreover, conventionally delivered drugs cannot be selectively transported to target cells.[14,15] Given these limitations, there is an urgent need for carriers capable of efficiently transporting therapeutic agents to their target tissues.

Nanomedicine, a field that combines nanotechnology and medicine, seeks to increase the efficacy of therapeutic substances in target tissues.[3,16,17] During pregnancy, nano-carriers could be used to transport drugs, peptides, or vaccines to the mother or fetus.[18–20] Before these materials can be deployed in the clinic, however, several issues must be resolved. First, it is

[a]*Laboratory of Nano-regenerative Medical Engineering, Department of Biomedical Science, College of Life Science, CHA University, 618, CHA Biocomplex, Sampyeong-Dong, Bundang-gu, Seongnam-si, 13488, Republic of Korea. E-mail: pkh0410@cha.ac.kr*
[b]*Laboratory of Molecular Genetics, Department of Biomedical Science, College of Life Science, CHA University, 629, CHA Biocomplex, Sampyeong-Dong, Bundang-gu, Seongnam-si, 13488, Republic of Korea. E-mail: shshim@cha.ac.kr*
[c]*Laboratory of Molecular Developmental Genetics, Department of Biomedical Science, College of Life Science, CHA University, Seongnam, Republic of Korea*
[d]*Department of Obstetrics and Gynecology, CHA Gangnam Medical Center, CHA University, Seoul, Republic of Korea. E-mail: chadh001@cha.ac.kr*
[e]*Fertility Center of CHA Gangnam Medical Center, CHA University, Seoul, Korea*

†Electronic supplementary information (ESI) available: Size analysis of NPs (TEM, and DLS), immunofluorescence image analysis, cellular uptake studies of fluorescence-labeled PNt, evaluation of damage and apoptosis in the placenta induced by PNt, and morphology, number, and weight of pups from pregnant mouse injected with saline or PNt. See DOI: 10.1039/d0bm00311e

‡These authors contributed equally to this work.

necessary to determine the efficiency with which nano-carriers can transport therapeutic agents to their targets, as well as the bioavailability of these agents in the body. In the context of pregnancy, the most important organ in this transport system is the placenta.[21–23] Located at the maternal–fetal interface, the placenta performs multiple functions throughout pregnancy: it structurally attaches the fetus to the uterine wall, provides oxygen and nutrients to the fetus, and removes fetal waste products.[24–28] In addition, it determines and regulates fetal exposure of xenobiotics, cytokines, hormones, or drugs. Thus, the maternal–placental–fetal interaction plays an essential role in pregnancy. Because mice and humans have similar placental transport mechanisms,[29,30] mice have been used as a developmental model for understanding human pregnancy. The mature placenta of mice, which is established by embryonic day (E) 10.5, consists of three layers:[31,32] the decidua, a layer of trophoblasts, and the labyrinth, which facilitates the exchange of materials between the maternal and fetal circulation. As the development proceeds, the villi of fetal blood vessels in the placenta branch densely to accommodate the increased requirements of the growing fetus.[32,33] Second, the side effects of transported nanoparticles (NPs), in particular their toxicity, must be determined. Developmental toxicity can result in disorders of pregnancy, including abortion, spontaneous preterm birth, or preeclampsia, thereby indirectly harming the offspring or inducing genetic aberration.[34–36] To

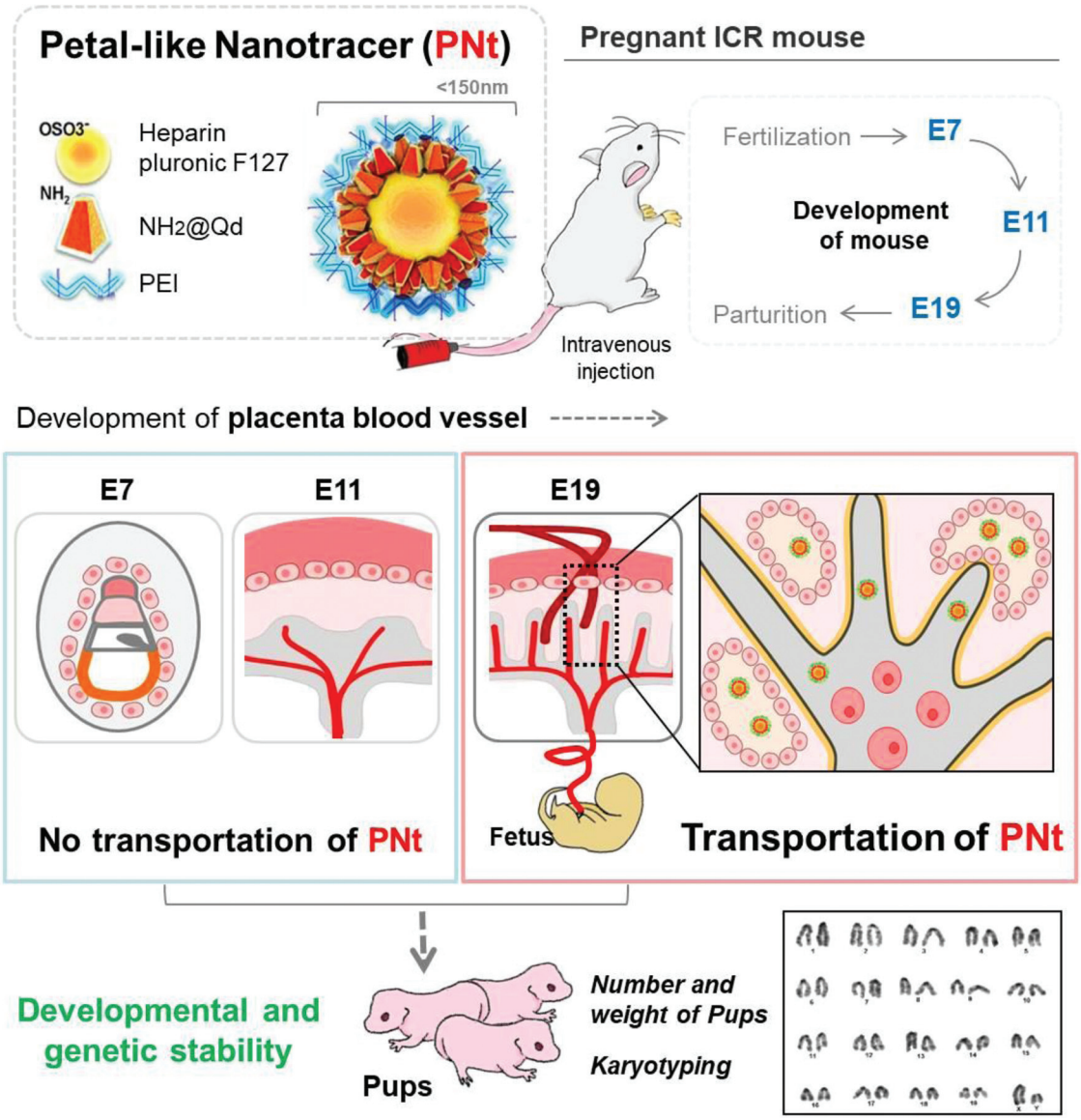

Scheme 1 Quantum dot (QD)-based nanoparticles composed of heparinized F127 gel and polyethylenimine (PEI), named petal-like nanotracers (PNts), were injected to pregnant ICR mice on embryonic day (E)7, E11, and E19 *via* the tail vein. The PNt transport depended on the stage of placental blood vessel development. At E19 (the late phase of embryonic development), but not at E7 or E11, PNts were transported from maternal to fetal blood vessels in the placenta. Pups from dams treated with PNts at all stages were genetically stable and exhibited no aberrations.

date, the reproductive and developmental toxicities of NPs have not been examined in detail. Such studies are necessary to evaluate the safety of pharmaceutical drugs.

In this study, we examined the effects of quantum dot (QD)-based nanoparticles in mice. Because QDs are toxic inorganic nanoparticles, we used QDs conjugated with amine groups, which were modified with heparin Pluronic F127 and polyethyleneimine (PEI); based on their morphology, we refer to the resultant particles as petal-like nanotracers (PNts). We sought to determine the biodistribution and effects of PNts in pregnant mice, especially in the placenta, following intravenous injection of the particles at three different stages of pregnancy (E7, E11, and E19). To obtain clinically useful information, we administered optimal doses of NPs.[37,38] Using Xenogen imaging and confocal laser microscopy, we determined the localization of PNts within the fetus and placenta at each stage of placental development. To investigate nanotoxicity, we monitored the developmental and genomic effects (genotoxicity) of PNts in the fetus, based on the number, morphology, biological status, and karyotype of pups (Scheme 1).

2. Materials and methods

2.1. Fabrication of PNts

In the following order, 0.5 ml Qdot® 655 ITK amino (PEG) QDs, 1 ml PEI, and 20 μg pDNA were mixed with heparin Pluronic F127 gel. Synthesis of heparin Pluronic F127 gel was carried out as described previously.[37,38] PNts were generated by electrostatic interaction in a 2 : 1 mixture of heparin Pluronic F127 gel and QDs.

2.2. Characterization of PNts

The hydrodynamic diameter of PNts was measured with a Zetasizer Nano ZS instrument (Malvern Incorporated, Malvern, UK). NPs were dispersed in de-ionized water, and 20 measurements were made. The morphology and distribution of PNts was visualized by TEM (H-7600, Hitachi, Tokyo, Japan) and AFM (NanoWizard II, JPK Instruments, Berlin, Germany). The samples were coated onto carbon film on 200 mesh copper grids (Electron Microscopy Science, Hatfield, PA, USA), dried overnight at room temperature, and visualized by TEM (ARM200F, JEOL, Tokyo, Japan).

2.3. Tracking PNts after IV injection (*in vivo* imaging)

To detect PNt QDs, *in vivo* imaging was performed using an IVIS Imaging System 200 (Xenogen, Perkin Elmer, Santa Clara, CA, USA) equipped with a Cy5.5 filter (excitation wavelength, 640 nm; emission wavelength, 695–770 nm).

To prepare a PNt, first, QD-encapsulating heparinized self-assembled nanogels (1 : 0.5) were prepared by dissolving 10 mg of heparinpluronic nanogels (10 mg ml^{-1}) in 1 ml of de-ionized water, adding 0.5 mL of QDs, and stirring. After that, QD-encapsulating heparinized nanogels were coated with 1 ml PEI. 10 μl of the PNt thus prepared was added to 100 μl of saline and then dispersed and injected. Pregnant ICR mice (E7, E11, and E19; n = 3 each; Orient-Bio, Seongnam, Korea) were injected with PNts in PBS *via* the tail vein and sacrificed 1 hour later; organs including liver, kidneys, and reproductive organs (uterus, placenta, and fetus) were excised for analysis.

All animal procedures were performed in accordance with the Guidelines for Care and Use of Laboratory Animals of CHA University and the experiments were approved by Institutional Animal Care and Use Committee (IACUC) of CHA. To trace PNts, the organs were monitored using a Xenogen imaging system.

2.4. Histological and immunofluorescence analysis

Excised organs were fixed with 4% paraformaldehyde (PFA) overnight, washed with PBS three times for 5 min each, and dehydrated with 10% sucrose overnight. Dehydrated organs were embedded in an optimal cutting temperature (OCT) compound (TISSUE-TEK 4583, Sakura Finetek Inc., Torrance, CA, USA) and sliced into sections (10 μm thick) using a cryotome (HM 525; Thermo Fisher Scientific, Waltham, MA, USA). After hydration, the sections were fixed and stained with hematoxylin (HHS16, Sigma Aldrich, St Louis, MO, USA) and eosin (HT110116, Sigma Aldrich) according to a standard protocol.

The fixed sections were permeabilized with 0.1% Triton X-100. After incubation with 1% BSA for 1 h, anti-Ki67 (sc23900, Santa Cruz Biotechnology, Dallas, TX, USA) and anti-caspase-3 (ab44976, Abcam) antibodies were added, and the samples were incubated overnight. After washing, secondary antibodies conjugated with Alexa Fluor 488 (1 : 1000 dilution) and Alexa Fluor 555 (1 : 1000 dilution) were applied for 0.5 h, followed by DAPI staining for 10 min. The sections were mounted in mounting solution (Dako Cytomation) and visualized by confocal fluorescence microscopy (LSM 880 META, Zeiss, Germany).

2.5. Western blotting analysis

For analysis of placental proteins, the tissue was homogenized in radioimmunoprecipitation (RIPA) buffer, and the lysates (30 μg) were separated on 8–10% SDS-PAGE gels and blotted onto membranes. The blots were incubated with primary antibodies and HRP-conjugated secondary antibodies (Bio-Rad, Hercules, CA, USA). The signals were detected on films using enhanced chemiluminescence (Amersham Pharmacia; GE Healthcare, Pittsburgh, PA, USA).

2.6. Isolation of neonatal fibroblasts

Embryos dissected from their dams at E7, E11, or E19 were cut into pieces with 0.05% collagenase IV solution (Invitrogen Life Technologies) and incubated in a shaking incubator for 1 h at 37 °C. The solution was filtered through a nylon cell strainer with 100 μm pore size (Corning Incorporated, Corning, NY, USA) and washed twice with Dulbecco's PBS (DPBS). The resultant cells were re-suspended in DMEM with high glucose (Hyclone) supplemented with 20% fetal bovine serum (FBS; Invitrogen Life Technologies) and 1% penicillin–streptomycin (Invitrogen Life Technologies), and then seeded into a 100 mm dish.

2.7. Membrane staining

The sections were stained with the lipophilic tracer 3,3′-dioctaecyloxacarbocyanine perchlorate (DIO, Sigma, St Louis, MO, USA) and DAPI for 3 min each, and then visualized by confocal fluorescence microscopy.

2.8. FACS analysis

Fibroblasts isolated from each pup were detached with trypsin/EDTA buffer (Invitrogen Life Technologies) and centrifuged at 1300 rpm for 3 min. The cells were washed twice with DPBS and suspended with 0.1% BSA. The resultant suspension was analyzed using a Guava EasyCyte System (Guava Technologies, Hayward, CA, USA); a total of 10 000 cells were analyzed to detect PNts.

2.9. Karyotyping

Karyotype analysis *via* G-banding was performed according to standard procedures. In brief, the cells were treated with KaryoMAX Colcemid Solution (Thermo Fisher Scientific) for 3 h, incubated with a hypotonic solution for 30 min, harvested by scraping, and centrifuged. Cell suspension in fixation buffer (3 : 1, methanol : acetic acid) was spread on the prepared slides, washed with 50% nitric acid, and kept in cold distilled water. Chromosomes were stained with Giemsa for 15 min, and a minimum of 20 banded metaphase cells were imaged and analyzed per group.

2.10. Statistical analysis

Data represent the means of at least three independent experiments ± SD. Statistical analyses were performed using the two-tailed Student's *t*-test; differences were considered to be significant at $p \leq 0.05$, and *p*-values are shown in figures as needed.

3. Results and discussion

3.1 Synthesis and characterization of petal-like nanotracers (PNts)

Fig. 1A shows a brief illustration of the flow of PNt tracking. PNts are composed of QD, PEI, and heparinized Pluronic 127 nanogel. The morphology and size (almost 20 nm) of the QDs are shown in Fig. S1.† The morphology and distribution of PNts were observed by transmission electron microscopy (TEM), which depicts flower-shaped nanoparticles composed of petals in a single layer (Fig. S1B† and Fig. 1B). The presence of the components of PNt, cadmium (Cd) in the QDs and sulfur (S) in the heparinized gel, were confirmed by elemental mapping by energy-dispersive X-ray spectroscopy (EDS) (Fig. 1B). The diameter of each PNt was 171 nm on average, and the material was monodisperse, as determined by DLS (Fig. 1C). The fluorescence intensity of QDs in complex with heparinized gel was similar to that of QDs alone, indicating that the QDs could be effectively detected by Xenogen (Fig. 1D). After exposure of NH @ QD and PNts to MSCs for 6 hours, survival was observed by varying the culture time. As a result of CCK-8 analysis of hMSCs, the cells were viable for all the time (Fig. S2†). In addition, PNts were slightly more stable in the hMSCs than NH @ QD for all the time.

PNts were intravenously injected into pregnant mice on embryonic day 19 (E19). After 1 h, the organs (liver, kidneys, ovaries, uterus, placenta, and fetus) were harvested and detected using a Xenogen imaging system (Fig. 1E). In addition, the organs were sectioned and visualized by confocal laser microscopy (Fig. S3†). After manipulating physicochemical properties (*i.e.*, size, morphology, and surface chemistry) to make the PNts suitable for safe tracing in the body, we applied them in mice.

Previous studies of disorders that arise during pregnancy have concentrated on improving the efficacy and delivery efficiency of drugs while decreasing their side effects in the body.[6,39–42] Treatments for mothers are focused on developing agents that are delivered efficiently to the intended organs without crossing the placenta to the fetus; on the other hand, drugs for the offspring are focused on efficient transport to the fetus without persistence in maternal compartments.[39,43,44] Recently, NPs have been investigated as a means of efficiently and safely delivering drugs during pregnancy. Specifically, multiple studies have been performed using liposomes composed of phospholipid bilayers, which have been approved by the Food and Drug Administration and are already used to treat a wide range of diseases, including cancers and infections. These include liposomes conjugated to oxytocin receptor antibodies and loaded with tocolytic drugs (indomethacin, nifedipine, salbutamol, and rolipram),[45–47] or decorated with tumor-homing sequences (CGKRK and iRGD; binding to the surface of mouse placenta) to target the placenta.[48] In addition, other NPs using poly(glycidyl methacrylate)(PGMA),[49] dendrimers,[50,51] silver NPs,[52–54] silica,[55] or quantum dots[37,38,56,57] have been used to deliver therapeutic agents to pregnant mice. By manipulating the properties of NPs (size, surface charge, surface functionalities, *etc.*), it is possible to adjust the loading, release, and targeting of drugs, as well as to regulate whether they cross the placenta during pregnancy.

3.2 Assessment of PNt biodistribution in organs from pregnant mice

Before tracking PNts *in vivo*, we traced them *in vitro* by confocal laser microscopy. In these experiments, PNts were internalized into human mesenchymal stem cells (hMSCs) and then detected after 4 hours by membrane staining (Fig. S4†). Almost all hMSCs took up PNts around the nucleus. To quantitatively assess PNt biodistribution in mice at three different stages of pregnancy (E7, E11, and E19), the organs (liver, kidneys, and reproductive organs: uterus, placenta, and fetus) were collected 1 h later and monitored by Xenogen imaging (Fig. 2A). Using the Cy5 filter (excitation, 610 nm; emission, 655 nm), PNts were detected at high levels in lungs, liver, and kidneys. By contrast, PNts were observed in reproductive organs (uterus, placenta, and fetus) only at E19, but not at E7

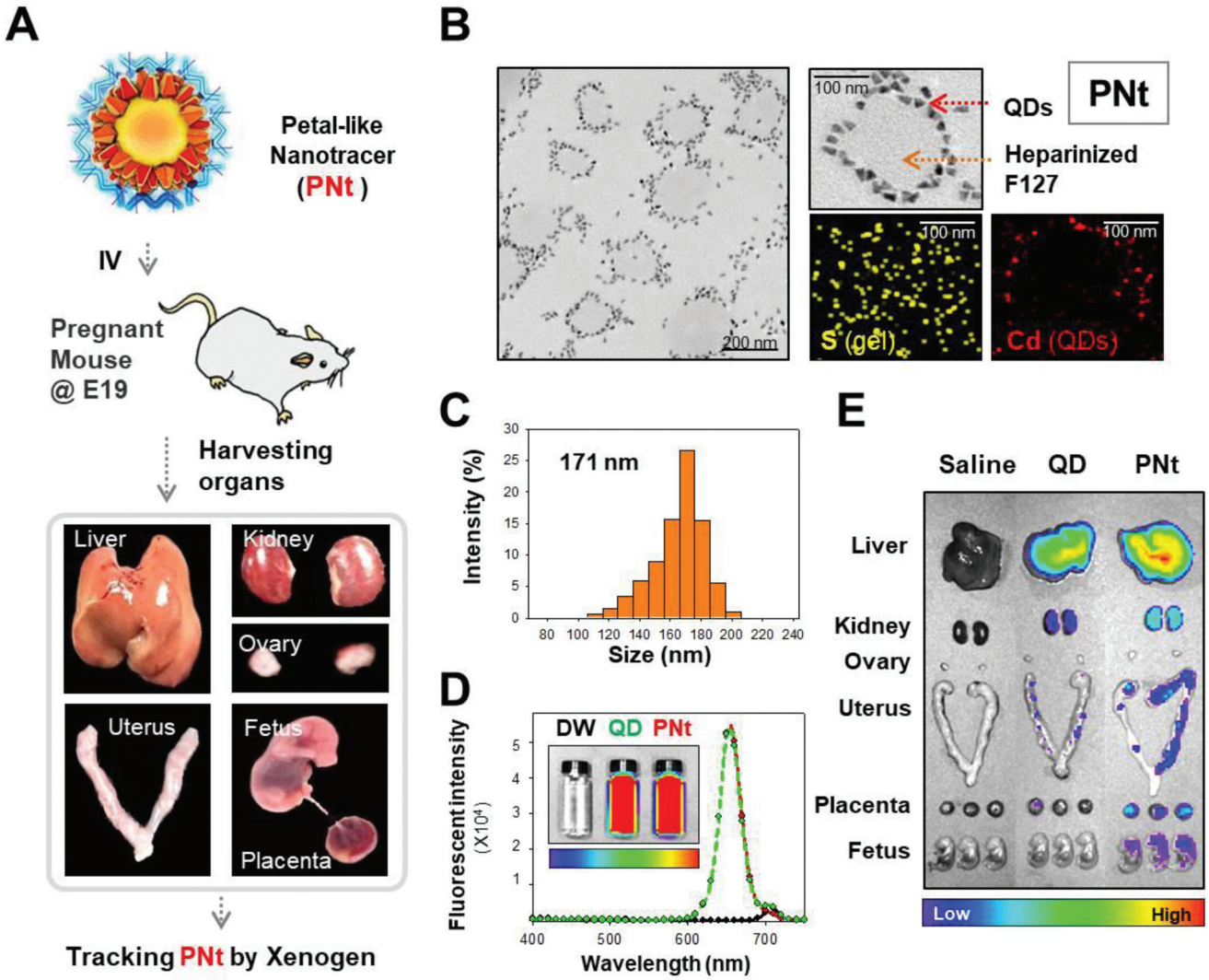

Fig. 1 Fabrication and characterization of petal-like nanotracers (PNts). Heparinized F127 gel, quantum dots (QDs), and polyethyleneimine (PEI) electrostatically interacted in that temporal order, yielding petal-like nanotracers (PNts), which were intravenously injected into pregnant mice (A). The morphology and distribution of PNts were visualized by transmission electron microscopy (TEM). Elemental mapping detected cadmium (Cd) in the QDs and sulfur (S) in the heparinized F127 gel (B). The sizes of PNts were measured by dynamic light scattering (DLS) (C). QD fluorescence was detected using a Xenogen system, making it possible to trace the PNts (D). The biodistribution of PNts in organs including liver, kidneys, ovaries, uterus, placenta, and fetus were detected by Xenogen (E).

or E11 (Fig. 2B). To observe the distribution of PNts in relation to nuclei, the tissue samples were fixed, sectioned, counter-stained with DAPI, and then subjected to confocal imaging (Fig. 2C). As in Fig. 2B, PNts were detected in the liver and kidneys regardless of stage, but in reproductive organs only at E19.

Recently, we developed modified QD-based nanoparticles (QD-NPs, named sunflower-type nanogels) with an appropriate size and surface functionalities to exhibit mono-dispersity and effective gene delivery[38] without introducing genetic problems *in vitro*. In this study, we demonstrated that modified QD-NPs called petal-like nanotracers (PNts) can cross the mouse placenta and distribute into the fetus during specific phases of development (E7, E11, or E19) without introducing developmental or genomic aberrations.

Due to the one-pass circulation time for blood in the mouse, the pregnant mice were sacrificed within 1 hour after PNt injection to observe the biodistribution of the NPs throughout the body. Xenogen imaging and confocal laser microscopy revealed that the capability of PNts to cross the placenta was influenced by embryonic and placental development.

3.3 Assessment of PNt biodistribution in reproductive organs

We confirmed the biodistribution of reproductive organs, including uterus and placenta, and fetus using Xenogen. This analysis showed that the PNt was present in the uterus at

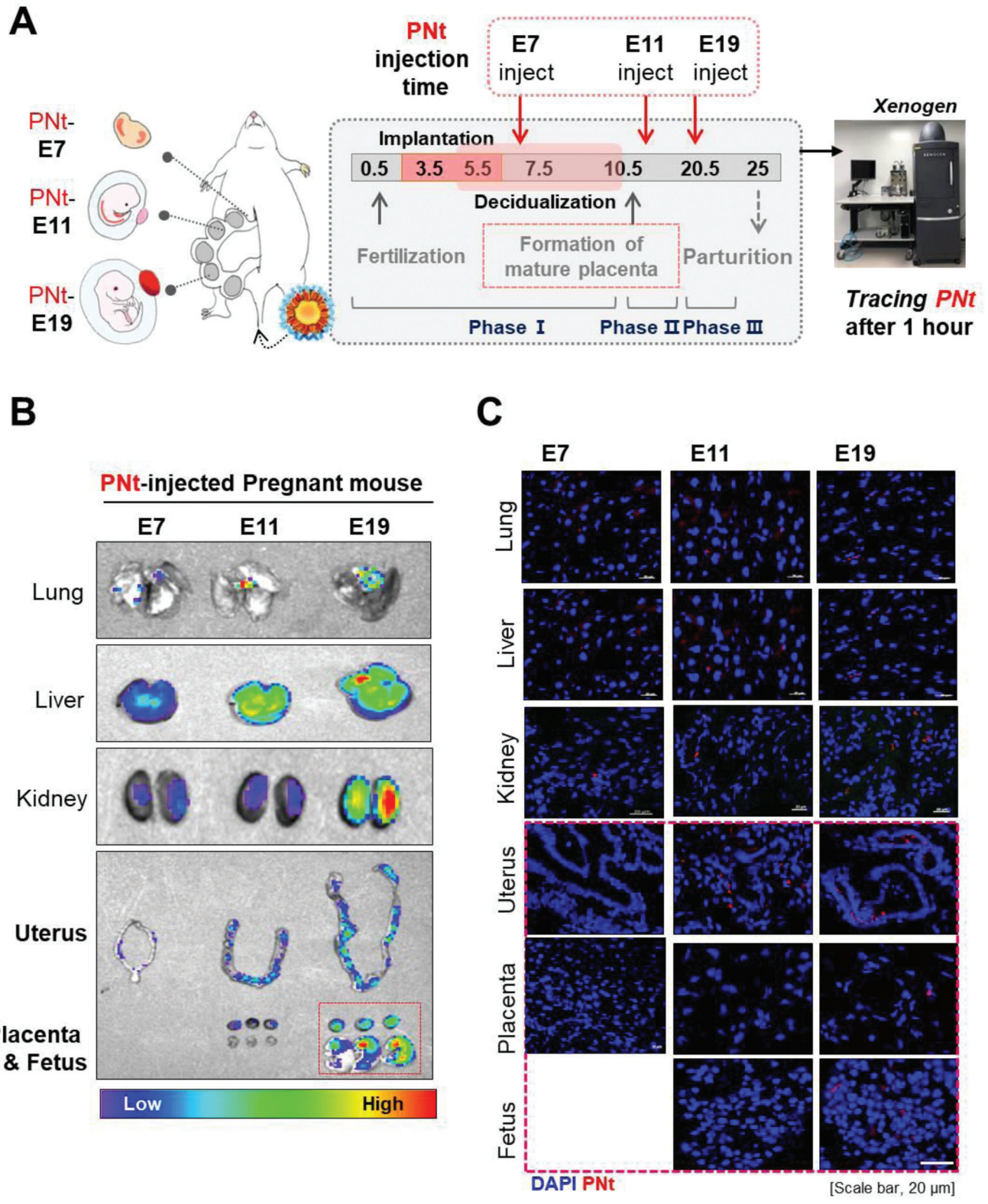

Fig. 2 Tracing PNts after tail vein injection into pregnant mice on embryonic day (E) 7, 11, and 19. Mouse development is divided into three phases (I, II, and III). In phase II, the mature form of the placenta is formed and gradually developed until the parturition. Pregnant mice at E7 (early), E11 (middle), and E19 (late) were injected with PNts *via* the tail vein and sacrificed 1 hour later; the organs (liver, kidneys, uterus, placenta, and fetus) were dissected for analysis. The organs were visualized by Xenogen imaging (A). The imaging results demonstrate that PNts were delivered to the reproductive organs (uterus, placenta, and fetus) only at E19 (B). The organs were fixed, dehydrated, and sectioned. The sections were stained with DAPI to detect nuclei, and subjected to confocal laser microscopy to detect PNts (C).

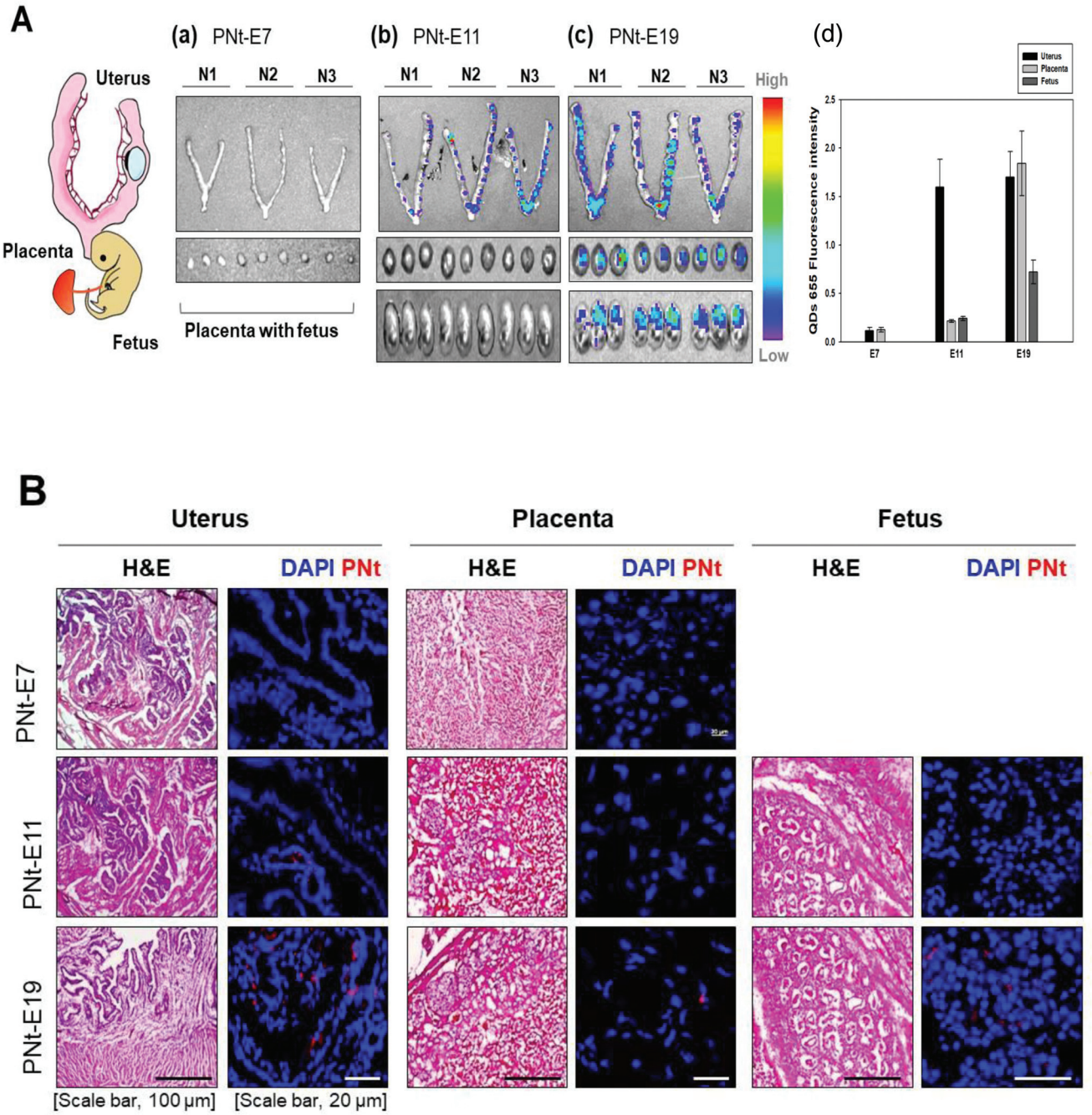

Fig. 3 Biodistribution of PNts in reproductive organs of pregnant mice. Reproductive organs, including the uterus, placenta, and fetus, were dissected from pregnant mice on E7, E11, and E19 (n = 3 each), and PNts were detected by Xenogen imaging (A). After that, the organs were fixed, dehydrated, and sectioned for H&E staining and confocal laser microscopy (B).

E11, and was subsequently transported to the placenta and fetus at E19 (Fig. 3A). To confirm that the organ structure was normal, the organs were fixed, sectioned, and stained with hematoxylin and eosin. We also observed the organ sections by confocal laser microscopy; this method confirmed the presence of PNts in the uterus at E11, and in the uterus, placenta, and fetus at E19 (Fig. 3B). These results indicate that PNts were transported into the fetus to a greater extent as development progressed.

3.4 Assessing the development of the placenta as a function of the phase of pregnancy, and determination of organ damage after PNt injection

To assess fetal development and damage to reproductive tissue, placentas were dissected from pregnant mice at E7, E11, and E19, and analyzed (Fig. 4A). The image of the placenta in Fig. 4B and immunofluorescence staining for CD31 (a blood vessel marker, Fig. S5†) showed that organ size and

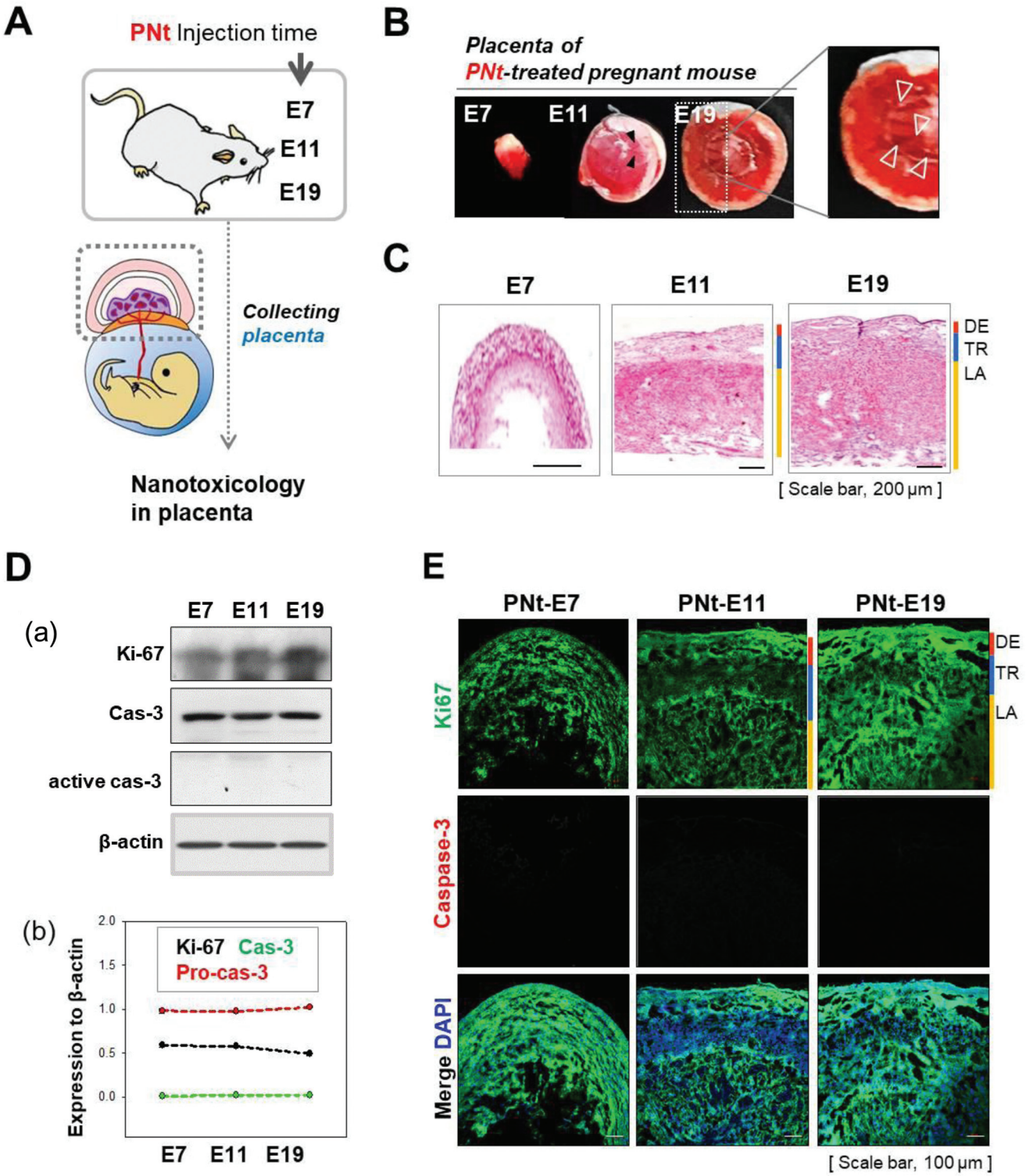

Fig. 4 Evaluation of damage and apoptosis in the placenta due to PNt exposure. One hour after injection of PNts into pregnant mice on E7, E11, and E19, placentas were dissected to evaluate the damage caused by the NPs (A). Blood vessels in the placenta matured over the course of development (B). In addition, the structure of the placenta developed extensively to a degree that depended on embryonic day (C). Western blotting analysis (D) and immunofluorescence analysis (E) of a proliferation marker (Ki67) and an apoptotic marker (caspase-3) revealed no dramatic apoptosis in the placenta at any developmental stage.

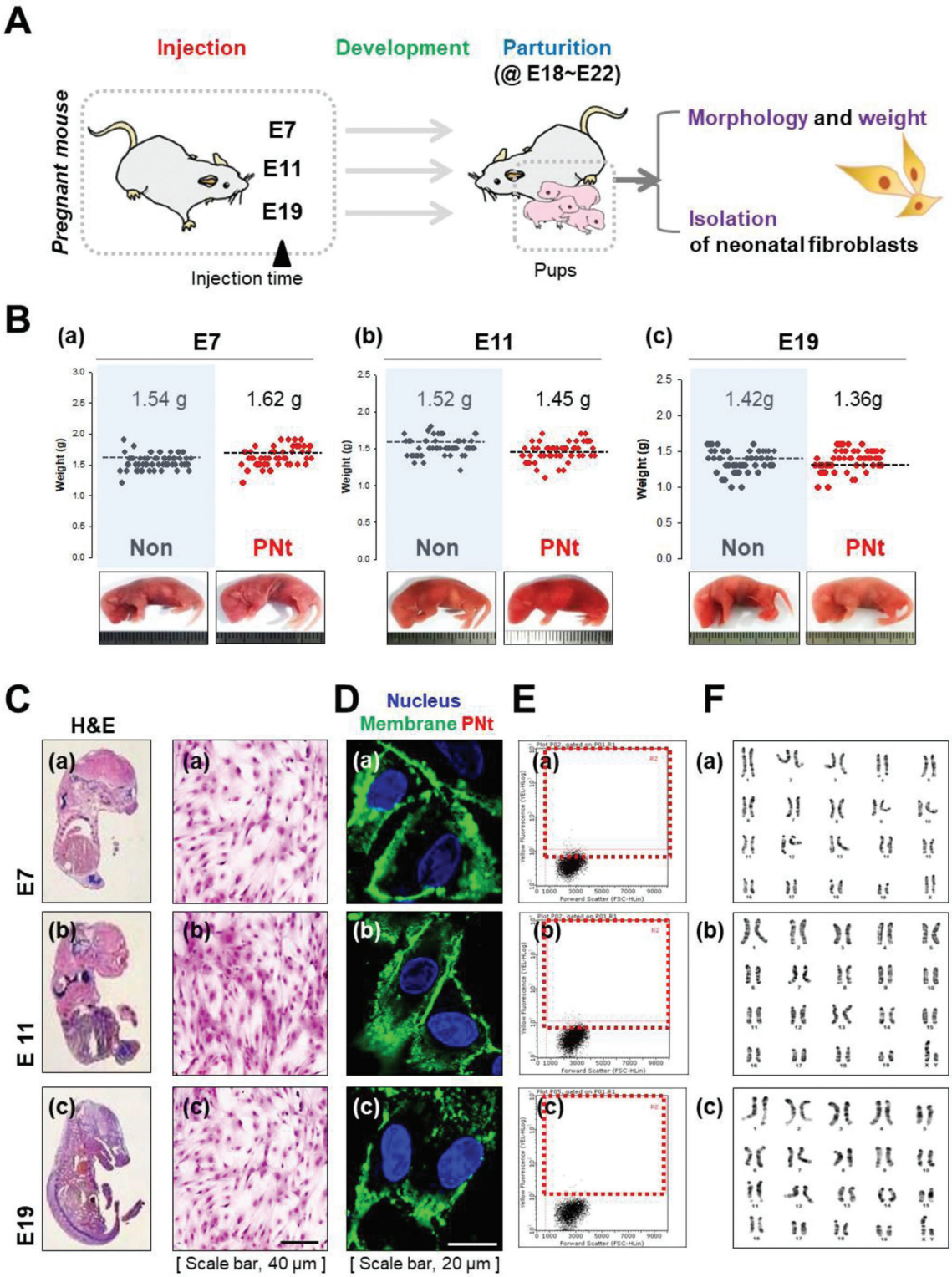

Fig. 5 Assessment of residual PNts and chromosomal stability in pups from PNt-treated dams. Pups from pregnant mice injected with saline or PNt on E7, E11, or E19 were analyzed to assess the level of residual PNts, as well as genetic stability (A). Weight of pups from pregnant mice injected with saline or PNts on E7, E11, or E19 (B). Representative images of pups and isolated primary fibroblasts from each group (C) were stained with hematoxylin (nucleus) and eosin (cytosol). Images of cultured fibroblasts, stained with DiO (green) and DAPI (blue) (D) and subjected to FACS analysis, show that cultured fibroblasts did not contain residual PNts (E). Karyotyping of primary cultured fibroblasts derived from one pup from each group revealed that PNts do not induce genomic instability (F).

vascularization increased as development progressed. Placental development is illustrated by the development of labyrinth, as revealed by H&E staining (Fig. 4C). Western blotting analysis (Fig. 4D) confirmed that Ki67 (a proliferation marker) was present in the placenta, and caspase-3 (an apoptosis marker) was absent, at all phases of pregnancy. Double immunofluorescence revealed positive staining for Ki67 and caspase-3 (Fig. 4E). When pregnant mice at E19 were injected with saline, QDs, or PNts, caspase-3 was not detected in all placenta (Fig. S6†).

The mature placenta of the mouse, which forms at E10.5, consists of three layers: the labyrinth, spongiotrophoblast, and maternal decidua. The labyrinth, the inner compartment of the placenta, contains the villi where nutrients and oxygen pass from the maternal to the fetal side during development.[23] The villi begin to form at E8.5 from allantois with thickening of the labyrinth for creating the space in the labyrinth of the interactions between maternal and fetal blood. The placenta has multifaceted functions, serving as a barrier to passage of nutrients and small molecules (including drugs and vaccines) between the mother and fetus.[32] In this study, the PNts crossed the placenta starting at the middle phase of embryonic development (E11) and were detectable in the fetus in the late phase (E19), at a time when the villi structure in the labyrinth was highly developed. By contrast, in the early phase (E7), when the structure was less developed, the PNts migrated only to the uterus. In the middle phase (E11), when the structures had assumed their mature form but were less vascularized than in the late phase (E19), PNts were transported to the placenta, but not to the fetus. PNt-treated placentas were not damaged, as shown by double immunofluorescence staining for Ki67 and caspase-3.

3.5 Identification of residual PNt and chromosomal stability in pups after injection

To evaluate the safety of PNts, pups from dams injected with saline or PNts at each embryonic stage were randomly selected and analyzed to assess whether they had developed normally (Fig. 5A). First, we identified the morphology, number, and weight of pups in each group (Fig. 5B). Pups of saline- and PNt-injected dams were born in similar numbers (E7, E11, and E19; 16, 15, and 16 on average), did not exhibit morphological abnormalities, and had similar body weights (saline- *vs.* PNt-injected mice at E7, E11, and E19; 1.54 g *vs.* 1.62 g, 1.52 g *vs.* 1.45 g, and 1.42 g *vs.* 1.36 g). Overall, pups from dams treated with saline or QDs at E7, E11, or E19 did not differ significantly in terms of morphology, number, and weight (Fig. S7†). To confirm genetic stability, fibroblast isolated f QD-encapsulating heparinized self-assembled nanogels (1 : 0.5) were prepared by dissolving 10 mg of heparinpluronic nanogels (10 mg ml^{-1}) in 1 ml of de-ionized water, adding 0.5 mL of QDs, and stirring.

To prepare sunflower-type nanogels, QD-encapsulating heparinized nanogels were coated with 1 ml PEI. From pups in each group were cultured (Fig. 5C). Confocal imaging (Fig. 5D) and FACS analysis (Fig. 5E) revealed that pup-derived fibroblasts did not contain PNts, and karyotyping indicated that all chromosomes were normal (Fig. 5F).

In this study, the embryonic days in mice are E7, E11, E19 ±1 day, corresponding to the early, middle, and late stages of human pregnancy. Since many drugs pass through the placenta and pass to the fetus, the selection and use of safe drugs during pregnancy is important. PNts show that the placenta is not delivered to the fetus in the incomplete state (E7), so it can be used to treat diseases of pregnant mice. However, PNts can be delivered to the fetus in E19 (late pregnancy) due to the development of the placenta, so it is preferable to administer the lowest dose of the dose range to minimize drug exposure to the fetus.

Collectively, these results suggest that it would be possible to regulate the final destination (organs) of injected nanoparticles bearing drugs, peptides, or genes by regulating the time when the NPs are introduced into the pregnant mouse. The nano-based delivery system may consider drug treatment of nanoparticles to be suitable for the number of weeks of pregnancy. Furthermore, we confirmed that pups from dams injected with PNts were normal, as reflected by their number, weight, and karyotype. As shown in Fig. 5 and Fig. S7,† PNts did not cause the offspring to have genetic aberrations or biological disorders. Thus, modified QD-NPs, which can be transported into the fetus, do not affect the status of the fetus or parturition even though they persist in the mother's organs. Taken together, our findings suggest that QD-based nanoparticles could be safely applied to pregnant individuals. By optimizing the conditions for administration of PNts, it should be possible to deliver genes or drugs selectively to mothers and their fetuses.

4. Conclusion

We analyzed the biodistribution of modified QD-based NPs (PNts) following intravenous injection into pregnant mice in the early, middle, and late phase of embryonic development. The results revealed that transport of these particles to the offspring depended on the placental stage of development. In the late phase of pregnancy, when the placenta contains highly branched blood vessels, PNts were transported to the fetus, but caused no abnormality in the number, appearance, or karyotype of the offspring. On the basis of these observations, we anticipate that PNts have the potential to serve as carriers of therapeutic agents for the treatment of the mother or fetus. Taken together, these findings have important implications for the development and application of QD-based NPs in pregnancy.

Conflicts of interest

The authors have declared that no competing interest exists.

Acknowledgements

This work was supported by National Research Foundation of Korea (NRF) grants funded by the Korean Government

(NRF-2020R1A2C3009783, NRF-2019R1A6A1A03032888, and NRF-2017M3A9C6061360).

References

1 L. A. Daalderop, B. V. Wieland, K. Tomsin, L. Reyes, B. W. Kramer, S. F. Vanterpool and J. V. Been, *JDR Clin. Trans. Res.*, 2018, **3**, 10–27.
2 S. F. Vanterpool, K. Tomsin, L. Reyes, L. J. Zimmermann, B. W. Kramer and J. V. Been, *Syst. Rev.*, 2016, **5**, 16.
3 S. Svenson, What nanomedicine in the clinic right now really forms nanoparticles?, *Wiley Interdiscip. Rev.: Nanomed. Nanobiotechnol.*, 2014, **6**, 125–135.
4 R. H. Beigi, *Obstet. Gynecol.*, 2017, **129**, 896–906.
5 L. Sobrevia, L. Myatt and G. Rice, *BioMed Res. Int.*, 2014, 937050.
6 J. A. Keelan, J. W. Leong, D. Ho and K. S. Iyer, *Nanomedicine*, 2015, **10**, 2229–2247.
7 R. W. Tolan, *Infect. Disord.: Drug Targets*, 2011, **11**, 424–425.
8 T. Iwamoto, *Biol. Pharm. Bull.*, 2013, **36**, 715–718.
9 R. H. He and R. Tao, *Adv. Exp. Med. Biol.*, 2017, **1010**, 219–245.
10 S. Y. Qin, A. Q. Zhang, S. X. Cheng, L. Rong and X. Z. Zhang, *Biomaterials*, 2017, **112**, 234–247.
11 L. Woods, V. Perez-Garcia and M. Hemberger, *Front. Endocrinol.*, 2018, **9**, 570.
12 A. M. Wagner, M. P. Gran and N. A. Peppas, *Acta Pharm. Sin. B*, 2018, **8**, 147–164.
13 W. D. Rollyson, C. A. Stover, K. C. Brown, H. E. Perry, C. D. Stevenson, C. A. McNees, J. G. Ball, M. A. Valentovic and P. Dasgupta, *J. Controlled Release*, 2014, **196**, 96–105.
14 S. C. van der Steen, R. Raave, S. Langerak, L. van Houdt, S. M. van Duijnhoven, S. A. van Lith, L. F. Massuger, W. F. Daamen, W. P. Leenders and T. H. van Kuppevelt, *Eur. J. Pharm. Biopharm.*, 2017, **113**, 229–239.
15 D. Chen, S. Lian, J. Sun, Z. Liu, F. Zhao, Y. Jiang, M. Gao, K. Sun, W. Liu and F. Fu, *Drug Delivery*, 2016, **23**, 808–813.
16 X. Ma, Y. Zhao and X. J. Liang, *Acc. Chem. Res.*, 2011, **44**, 1114–1122.
17 A. C. Anselmo and S. Mitragotri, *Bioeng. Transl. Med.*, 2016, **1**, 10–29.
18 I. V. Zhigaltsev, Y. K. Tam, A. K. Leung and P. R. Cullis, *J. Liposome Res.*, 2016, **26**, 96–102.
19 P. P. Desai, A. A. Date and V. B. Patravale, *Drug Discovery Today: Technol.*, 2012, **9**, e87–e95.
20 A. A. Manzoor, L. H. Lindner, C. D. Landon, J. Y. Park, A. J. Simnick, M. R. Dreher, S. Das, G. Hanna, W. Park, A. Chilkoti, G. A. Koning, T. L. ten Hagen, D. Needham and M. W. Dewhirst, *Cancer Res.*, 2012, **72**, 5566–5575.
21 M. Saunders, *Wiley Interdiscip. Rev.: Nanomed. Nanobiotechnol.*, 2009, **1**, 671–684.
22 M. Ruiz-Palacios, A. J. Ruiz-Alcaraz, M. Sanchez-Campillo and E. Larque, *Ann. Nutr. Metab.*, 2017, **70**, 16–25.
23 W. W. Hay Jr., *Horm. Res.*, 1994, **42**, 215–222.
24 L. D. Longo and L. P. Reynolds, *Int. J. Dev. Biol.*, 2010, **54**, 237–255.
25 A. E. Guttmacher, Y. T. Maddox and C. Y. Spong, *Placenta*, 2014, **35**, 303–304.
26 J. Jeevanandam, A. Barhoum, Y. S. Chan, A. Dufresne and M. K. Danquah, *Beilstein J. Nanotechnol.*, 2018, **9**, 1050–1074.
27 S. Lager and T. L. Powell, *J. Pregnancy*, 2012, 179827.
28 D. Newbern and M. Freemark, *Curr. Opin. Endocrinol., Diabetes Obes.*, 2011, **18**, 409–416.
29 M. R. Dilworth and C. P. Sibley, *Placenta*, 2013, **34**, S34–S39.
30 F. Soncin, M. Khater, C. To, D. Pizzo, O. Farah, A. Wakeland, K. A. N. Rajan, K. K. Nelson, C. W. Chang, M. Moretto-Zita, D. R. Natale, L. C. Laurent and M. M. Parast, *Development*, 2018, **145**, 156273.
31 P. Georgiades, A. C. Ferguson-Smith and G. J. Burton, *Placenta*, 2002, **23**, 3–19.
32 E. D. Watson and J. C. Cross, *Physiology*, 2005, **20**, 180–193.
33 E. Solomon, R. Avni, R. Hadas, T. Raz, J. R. Garbow, P. Bendel, L. Frydman and M. Neeman, *Proc. Natl. Acad. Sci. U. S. A.*, 2014, **111**, 10353–10358.
34 M. I. Mohamed, M. K. Mohammad, H. R. A. Razak, K. Abdul Razak and W. M. Saad, *BioMed Res. Int.*, 2015, 183525.
35 J. Sun, Q. Zhang, Z. Wang and B. Yan, *Int. J. Mol. Sci.*, 2013, **14**, 9319–9337.
36 Y. Li, Y. Zhang and B. Yan, *Int. J. Mol. Sci.*, 2014, **15**, 3671–3697.
37 J. S. Park, S. W. Yi, H. J. Kim, S. M. Kim, S. H. Shim and K. H. Park, *Biomaterials*, 2016, **77**, 14–25.
38 J. S. Park, S. W. Yi, H. J. Kim, H. J. Oh, J. S. Lee, M. Go, S. H. Shim and K. H. Park, *Theranostics*, 2018, **8**, 5548–5561.
39 E. M. George, H. Liu, G. G. Robinson and G. L. Bidwell, *J. Drug Targeting*, 2014, **22**, 935–947.
40 Q. Wang, X. Zhuang, J. Mu, Z. B. Deng, H. Jiang, L. Zhang, X. Xiang, B. Wang, J. Yan, D. Miller and H. G. Zhang, *Nat. Commun.*, 2013, **4**, 1867.
41 B. Zhang, L. Tan, Y. Yu, B. Wang, Z. Chen, J. Han, M. Li, J. Chen, T. Xiao, B. K. Ambati, L. Cai, Q. Yang, N. R. Nayak, J. Zhang and X. Fan, *Theranostics*, 2018, **8**, 2765–2781.
42 H. Ragelle, F. Danhier, V. Préat, R. Langer and D. G. Anderson, *Expert Opin. Drug Delivery*, 2017, **14**, 851–864.
43 M. Feghali, R. Venkataramanan and S. Caritis, Pharmacokinetics of drugs in pregnancy, *Semin. Perinatol.*, 2015, **39**, 512–519.
44 R. Bajoria, S. Sooranna and R. Chatterjee, *Placenta*, 2013, **34**, 1216–1222.
45 K. J. Moise Jr., C. N. Ou, B. Kirshon, L. E. Cano, C. Rognerud and R. J. Carpenter Jr., *Am. J. Obstet. Gynecol.*, 1990, **162**, 549–554.
46 J. S. Refuerzo, J. F. Alexander, F. Leonard, M. Leon, M. Longo and B. Godin, *Am. J. Obstet. Gynecol.*, 2015, **212**(508), e501–e507.

47 R. D. Suarez, W. A. Grobman and B. V. Parilla, *Obstet. Gynecol.*, 2001, **97**, 921–925.
48 A. King, C. Ndifon, S. Lui, K. Widdows, V. R. Kotamraju, L. Agemy, T. Teesalu, J. D. Glazier, F. Cellesi and N. Tirelli, *Sci. Adv.*, 2016, **2**, e1600349.
49 D. Ho, J. W. Leong, R. C. Crew, M. Norret, M. J. House, P. J. Mark, B. J. Waddell, K. S. Iyer and J. A. Keelan, *Sci. Rep.*, 2017, **7**, 2866.
50 A. R. Menjoge, A. L. Rinderknecht, R. S. Navath, M. Faridnia, C. J. Kim, R. Romero, R. K. Miller and R. M. Kannan, *J. Controlled Release*, 2011, **150**, 326–338.
51 A. R. Menjoge, R. S. Navath, A. Asad, S. Kannan, C. J. Kim, R. Romero and R. M. Kannan, *Biomaterials*, 2010, **31**, 5007–5021.
52 Y. Lee, J. Choi, P. Kim, K. Choi, S. Kim, W. Shon and K. Park, *Toxicol. Res.*, 2012, **28**, 139–141.
53 L. Campagnolo, M. Massimiani, L. Vecchione, D. Piccirilli, N. Toschi, A. Magrini, E. Bonanno, M. Scimeca, L. Castagnozzi, G. Buonanno, L. Stabile, F. Cubadda, F. Aureli, P. H. Fokkens, W. G. Kreyling, F. R. Cassee and A. Pietroiusti, *Nanotoxicology*, 2017, **11**, 687–698.
54 C. A. Austin, T. H. Umbreit, K. M. Brown, D. S. Barber, B. J. Dair, S. Francke-Carroll, A. Feswick, M. A. Saint-Louis, H. Hikawa, K. N. Siebein and P. L. Goering, *Nanotoxicology*, 2012, **6**, 912–922.
55 S. R. Pinto, E. Helal-Neto, F. Paumgartten, I. Felzenswalb, C. F. Araujo-Lima, R. Martinez-Manez and R. Santos-Oliveira, *Artif. Cells, Nanomed., Biotechnol.*, 2018, **46**, 1–12.
56 M. Chu, Q. Wu, H. Yang, R. Yuan, S. Hou, Y. Yang, Y. Zou, S. Xu, K. Xu, A. Ji and L. Sheng, *Small*, 2010, **6**, 670–678.
57 N. Wu, Z. Zhang, J. Zhou, Z. Sun, Y. Deng, G. Lin, M. Ying, X. Wang, K. T. Yong, C. Wu and G. Xu, *Nanotheranostics*, 2017, **1**, 261–271.